

ANALYTIC EVALUATION OF THE LAMPF II BOOSTER CAVITY DESIGN*

C. C. Friedrichs, AT-5, MS H827
 Los Alamos National Laboratory, Los Alamos, NM 87545 USA

Summary

Through the past few decades, a great deal of sophistication has evolved in the numeric codes used to evaluate electromagnetically resonant structures. The numeric methods are extremely precise, even for complicated geometries, whereas analytic methods require a simple uniform geometry and a simple, known mode configuration if the same precision is to be obtained.

The code SUPERFISH, which is near the present state of the art of numeric methods, does have the following limitations: No circumferential geometry variations are permissible; there are no provisions for magnetic or dielectric losses; and finally, it is impractical (because of the complexity of the code) to modify it to extract particular bits of data one might want that are not provided by the code as written. This paper describes how SUPERFISH was used as an aid in derivating an analytic model of the LAMPF II Booster Cavity. Once a satisfactory model was derived, simple FORTRAN codes were generated to provide whatever data was required. The analytic model is made up of TEM- and radial-mode transmission-line sections, as well as lumped elements where appropriate. Radial transmission-line equations, which include losses, were not found in any literature, and the extension of the lossless equations¹ to include magnetic and dielectric losses are included in this paper.

Analytic Model Evolution

The LAMPF II Booster Cavity is tuned from ~50 to 60 MHz by varying the permeability of ferrite rings in the high-current end of the cavity. Perpendicular bias control of the ferrite is used to achieve this variation.²

The booster cavity geometry shown in Fig. 1. was designed using the rf cavity code, SUPERFISH. The analytic model for the gap end of this cavity is simply a uniform TEM transmission line terminated in a capacitor. The characteristic impedance of this TEM section was calculated from the ratio of the coaxial radii. The gap capacitance was derived from SUPERFISH data, and the length was obtained by a physical measurement from the gap to the neck region of the cavity (see Fig. 1).

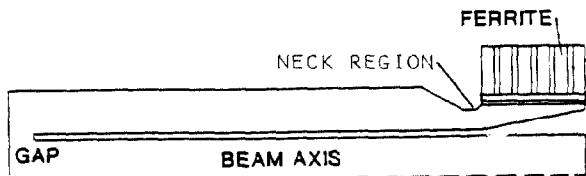


Fig. 1. Booster cavity geometry.

The analytic model for the ferrite end of the cavity is considerably more complicated. The SUPERFISH electric-field calculation of the ferrite end of the cavity is shown in Fig. 2. This figure suggests that the ferrite and insulator portions of the cavity should be modeled using radial transmission lines and the remaining portion, through the neck, by a uniform TEM

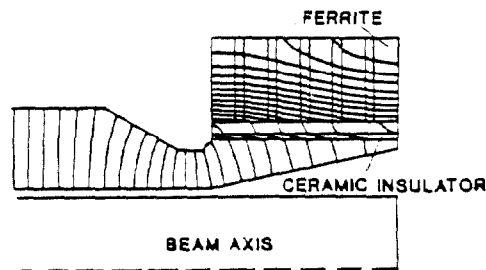


Fig. 2. Electric fields in the tuner end.

section. The resulting cavity analytic model is described by the following five distinct sections.

Radial Sections (Terminology as defined in Ref. 1.):

Section	Load Radius (in.)	Input Radius (in.)	Spacing (in.)	μ_r	ϵ_r
1	11.831	6.30	7.25	μ_1	13.456
2	6.30	5.76	7.25	1	1
3	5.76	5.51	7.25	1	10

$\mu_1 = (6\mu_r + 1.25)/7.25$, and μ_r is the relative permeability of the ferrite. This expression accounts for the spacers between the ferrites.

TEM Sections (Coaxial):

Section	Outer Radius (in.)	Inner Radius (in.)	Length (in.)	Z_0 (Ω)
4	5.468	3.543	5.87	26.04
5	6.890	3.543	28.58	39.90

Finally, the end of the fifth section is terminated in a 7.83-pF capacitor.

The parameters of transmission-line Sections 1, 2, 3, and 5 were determined from physical dimensions of the SUPERFISH model. The terminating capacitor was calculated from the SUPERFISH standing-wave voltage distribution along Section 5, and finally, as previously noted, the length and characteristic impedance of Section 4 were first estimated from physical dimensions, then adjusted to bring the whole model into agreement with SUPERFISH at both ends of the frequency range. The analytic model was evaluated by calculating the input impedance to Section 1 (its load impedance is the wall resistance of the end section), then placing that input impedance as the load impedance to the next section. Input impedances were successively calculated until the input impedance to Section 5, including the gap capacitance, was found. The imaginary part of this impedance should approach infinity for resonance to exist.

Lossy, Radial Transmission Lines

The treatment of lossy, TEM transmission lines is found in numerous texts and will not be discussed here. The extension of the lossless radial transmission-line equations¹ to include magnetic and/or dielectric losses follows, without proof because of space limitations.

These equations make use of the Bessel functions J_0 , J_1 , N_0 , and N_1 ; the argument of each is kr , where

*Work supported by Los Alamos National Laboratory Institutional Supporting Research and Development.

r = radius at which the function is being evaluated,

$$k = 2\pi f(\mu\epsilon)^{1/2}$$

μ = total permeability of the medium, and
 ϵ = total dielectric constant of the medium.

In the lossless case, the agreement is real and the functions are real. In the lossy case, k is modified as follows:

$$k = 2\pi f(\mu\epsilon)^{1/2} \left[\left(1 - \frac{1}{Q_m Q_e}\right) - j \left(\frac{1}{Q_m} + \frac{1}{Q_e}\right) \right]^{1/2}$$

where Q_m and Q_e are the magnetic and dielectric Q s of the medium, respectively. For high- Q values (>100),

$$k = 2\pi f(\mu\epsilon)^{1/2} \left[1 - j(0.5) \left(\frac{1}{Q_m} + \frac{1}{Q_e}\right) \right]$$

Because the argument is now complex, the functions will be complex. The functions, however, are evaluated using the same series expansions as if the argument were real. Definitions of those expansions are collected below.

$$J_0(kr) = 1 + \sum_{n=1}^{\infty} \frac{(-1)^n (0.5kr)^{2n}}{(n!)^2}$$

$$J_1(kr) = \sum_{n=1}^{\infty} \frac{-n(-1)^n (0.5kr)^{2n-1}}{(n!)^2}$$

$$N_0(kr) = 2\pi \left[\log_n \gamma + \log_n(0.5kr) + \sum_{n=1}^{\infty} \text{FN} \frac{(-1)^n (0.5kr)^{2n}}{(n!)^2} \right]$$

and

$$N_1(kr) = 2\pi \left[\frac{1}{kr} + \sum_{n=1}^{\infty} (n\text{FN} + 0.5) \frac{(-1)^n (0.5kr)^{2n-1}}{(n!)^2} \right]$$

where $\log_n \gamma = 0.5772157$ (Euler's constant),

and

$$\text{FN} = \log_n \gamma + \log_n(0.5kr) - \sum_{m=1}^n \left(\frac{1}{m}\right)$$

The radial transmission-line equations depend on Z_0 , θ and ψ . The equations for evaluating these parameters follow:

Define

$$\begin{aligned} R_{01} &= \text{Re}(J_0) - \text{Im}(N_0), & I_{01} &= \text{Im}(J_0) + \text{Re}(N_0) \\ R_{02} &= \text{Re}(J_0) + \text{Im}(N_0), & I_{02} &= \text{Im}(J_0) - \text{Re}(N_0) \\ R_{11} &= \text{Re}(J_1) - \text{Im}(N_1), & I_{11} &= \text{Im}(J_1) + \text{Re}(N_1) \end{aligned}$$

$\text{Re}()$ and $\text{Im}()$ designate the real and imaginary parts of a complex function, respectively,
 $R_{12} = \text{Re}(J_1) + \text{Im}(N_1)$, $I_{12} = \text{Im}(J_1) - \text{Re}(N_1)$;

as a general expression,

$$M_{ab} = [(R_{ab})^2 + (I_{ab})^2]^{1/2}$$

Then,

$$\begin{aligned} G_0 &= (M_{01}M_{02})^{1/2} \\ \alpha_0 &= \log(n)(M_{01}/G_0) \\ G_1 &= (M_{11}M_{12})^{1/2} \\ \alpha_1 &= \log(n)(M_{11}/G_1) \\ \phi_0 &= 1/2[\text{ARCTAN}(I_{01}/R_{01}) + \text{ARCTAN}(I_{02}/R_{02})] \\ \phi_1 &= 1/2[\text{ARCTAN}(I_{11}/R_{11}) + \text{ARCTAN}(I_{12}/R_{12})] \\ \beta_0 &= 1/2[\text{ARCTAN}(I_{01}/R_{01}) - \text{ARCTAN}(I_{02}/R_{02})] \\ \beta_1 &= 1/2[\text{ARCTAN}(I_{11}/R_{11}) - \text{ARCTAN}(I_{12}/R_{12})] \end{aligned}$$

Finally,

$$Z_0(kr) = (\mu/\epsilon)^{1/2} \left[1 - j(0.5) \left(\frac{1}{Q_m} - \frac{1}{Q_e}\right) \right] \frac{G_0 e^{j\phi_0}}{G_1 e^{j\phi_1}}$$

$$\theta(kr) = \alpha_0 + j\beta_0 \quad , \quad \text{and}$$

$$\psi(kr) = \alpha_1 + j\beta_1 \quad .$$

With Z_0 , θ , and ψ redefined for the lossy case, they can be used directly in the radial transmission-line Eq. 9-13 (13) page 400 of Ref. 1. Because θ and ψ are now complex, complex cosines and sines must be evaluated: (CCOS and CSIN in FORTRAN).

The Complete Analytic Model

Once the cavity analytic model was determined, the capacitively coupled amplifier was added. Figure 3 shows the amplifier arm as the vertical member. It also shows provisions for external loading through C_2 . The values of these lumped elements are tabulated below:

Element	Description	Value
C_1	Gap Capacitance	7.83 pF
C_2	External-load capacitor	4.095 pF
C_3	Amplifier output capacitance	60 pF
C_4	Coupling capacitor	20.58 pF
	External-load resistance	25 Ω

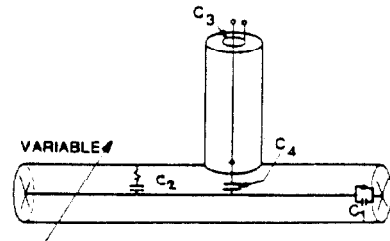


Fig. 3. Amplifier coupling model.

The equivalent beam-load impedance is added across C_1 . The amplifier arm is 21 in. long and its characteristic impedance is 37.7 Ω . The characteristic impedance of the horizontal section remains 39.9 Ω , with an outer radius of 6.89 in. and an inner radius of 3.543 in. The lengths that replace the 28.58-in. length of Section 5 of the cavity analytic model are as follows:

Section 4 to C_2 - 6.506 in.

C_2 to C_4 - 6.0 in.

C_4 to C_1 - 9.0 in.

Note that the cavity is shortened about 7 in. by the addition of the amplifier. Sections 1 through 4 of the cavity analytic model remain intact as the tuning variable.

The most significant parameter that can be calculated from the complete model is the rf amplifier load impedance. That is the impedance seen looking into the model at the terminals across C_3 . A scaled drawing of the resulting booster cavity and amplifier is shown in Fig. 4.

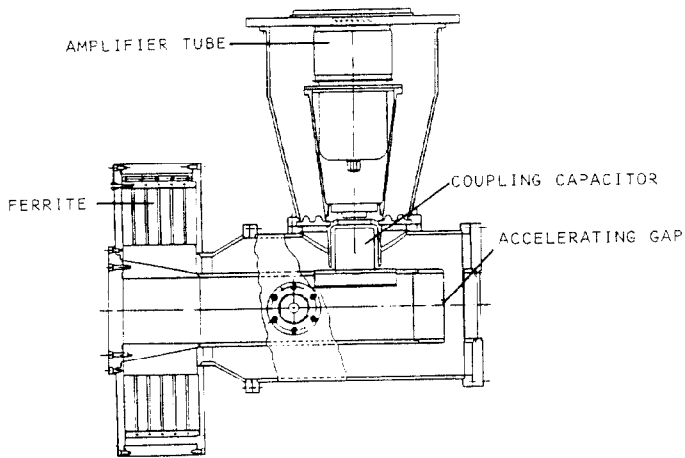


Fig. 4. Booster cavity and amplifier.

Calculation Results and Conclusions

Several FORTRAN codes were written based on the analytic models. The first code was used to optimize the ferrite dimensions. The second code was used to locate the amplifier and size the coupling capacitor. Another code was written that gave wall-loss heat distribution over the cavity. Peak and average power-dissipation density was mapped through the ferrite by another code. Finally, the amplifier plate load over the acceleration cycle was plotted.

The calculated results show that the cavity can be tuned from 50.3 to 59.2 MHz by varying the control current in the bias coils so that the relative permeability of the ferrite changes from 2.64 down to 1.43. The maximum rms dissipation density occurring in the ferrite during the accelerating cycle is 1.25 W/cm^3 , and the average over the cycle is 200 mW/cm^3 . The rf amplifier plate-load resistance stays within the limits 500 to 700 Ω . In the areas evaluated by these analytic techniques, the cavity-amplifier package design has a comfortable safety margin.

Acknowledgments

The author wishes to thank his colleagues, George Spalek and Roger Carlini, whose need for information prompted the work leading to this paper.

References

1. Simon Ramo and John R. Whinnery, "Fields and Waves in Modern Radio," (John Wiley and Sons, Inc. New York, Chapman and Hall Ltd. London 1953), 395-400.
2. W. R. Smythe, T. G. Brophy, University of Colorado, R. D. Carlini, C. C. Friedrichs, D. L. Grisham, G. Spalek, L. C. Wilkerson, Los Alamos National Laboratory, "RF Cavities with Transversely Biased Ferrite Tuning," these proceedings.